PCCP

ROYAL SOCIETY OF CHEMISTRY

PAPER

View Article Online
View Journal | View Issue

Cite this: *Phys. Chem. Chem. Phys.*, 2025, **27**, 21297

The primary photolysis of aqueous acrylate

Jan Thøgersen, Akriti Mishra, Tobias Weidner and Frank Jensen *

Received 7th August 2025,
Accepted 5th September 2025

DOI: 10.1039/d5cp03023d

rsc.li/pccp

We apply transient absorption spectroscopy supported by 2D-IR spectroscopy and density functional theory calculations to determine the primary photolysis of acrylate excited *via* the $\pi^*_{CO} \leftarrow \pi_{CO}$ transition at 200 nm. Upon photoexcitation, about half of the excited acrylate anions return to the ground state and relax to equilibrium in 5 ps primarily through intermolecular coupling between the carboxylate group and the surrounding water. The rest of the excited acrylate anions dissociate. Three dissociation channels have been identified. In one reaction, decarboxylation of acrylate forms CO_2 and CH_2CH^-. CH_2CH^- is protonated by water and forms ethene, C_2H_4, in <0.8 ps. In the second reaction, the excited acrylate anions dissociate to $H_2C{=}CHO^-$ and CO. In about 20 ps, $H_2C{=}CHO^-$ picks up a proton from water to produce vinyl alcohol, $H_2C{=}CHOH$. A third dissociation channel forms $H_2C{=}CHO^\bullet$ and CO^-. $H_2C{=}CHO^\bullet$ abstracts a hydrogen atom from water and forms vinyl alcohol. Vinyl alcohol will tautomerize to acetaldehyde, but this occurs on a time scale longer than the experimental observation time of 0.56 ns.

Introduction

The recent discovery of photon emission accompanying electric discharges between oppositely charged microdroplets in water sprays may potentially revolutionize our understanding of the chemistry near the surface of lakes and oceans.[1,2] The maximum energy of these micro-lightnings is somewhere between 12.1 eV and 12.5 eV and water sprays are thus capable of dissociating and ionizing most molecules. Consequently, the photochemistry of the biosphere is not necessarily limited to reactions induced by the sunlight passing through the ozone layer (4 eV) but may also include reactions requiring far more energy.

However, the photo-absorption of water sets in around 195 nm (6.4 eV)[3] and this defines an upper limit for the photon energies capable of exciting molecules in bulk aqueous solutions. Consequently, the photolysis of saturated carboxylates can only occur through photoexcitation of their weak $\pi^*_{CO} \leftarrow n_O$ transition from the oxygen lone pair electrons to the anti-bonding π^* orbitals of the carboxylate, while the absorption from water prevents the much stronger $\pi^*_{CO} \leftarrow \pi_{CO}$ excitation of the carboxylate π electrons.[4] In contrast to the saturated carboxylates, the conjugation in unsaturated carboxylates reduces the energy gap between the bonding π and anti-bonding π^* orbitals, making the latter accessible to photoexcitation in water through the strong $\pi^*_{CO} \leftarrow \pi_{CO}$ transition. The photolysis of unsaturated carboxylates in aqueous solution can therefore occur by excitation of bonding π_{CO} electrons as well as non-bonding n_O electrons into the anti-bonding π^*_{CO} orbital. Excitation of a π_{CO} electron makes the π-orbital accessible to repopulation by non-bonding electrons from the higher lying n_O state. If such Auger–Meitner repopulation occurs before the photolysis has time to proceed, the initial $\pi^*_{CO} \leftarrow \pi_{CO}$ photoexcitation of the unsaturated carboxylate essentially becomes a $\pi^*_{CO} \leftarrow n_O$ excitation, but with the strong transition probability provided by the initial $\pi^*_{CO} \leftarrow \pi_{CO}$ transition.[5] Following this line of argument, the photolysis dynamics of aqueous unsaturated carboxylates by $\pi^*_{CO} \leftarrow \pi_{CO}$ excitation may resemble that of $\pi^*_{CO} \leftarrow n_O$ excitation of aqueous saturated carboxylates at the same excitation energy.

Acrylate (2-propenoate) is the smallest unsaturated carboxylate, consisting of an ethenyl group connected directly to a carboxylate group. Due to natural sources as well as vast industrial production, acrylate is ubiquitous in the biosphere and thus also in seawater and atmospheric aerosols.[6,7] The literature on acrylate's photochemistry is sparse but data are available for acrylic acid.[8–10] According to calculations by Shemesh and Gerber,[9] the photochemistry of acrylic acid results from a weak $\pi^*_{CO} \leftarrow n_O$ transition with an excitation energy of 4.40 eV (282 nm) and an oscillator strength of 0.001 and a stronger $\pi^*_{CO} \leftarrow \pi_{CO}$ transition of mixed $\pi^*_{C=O}/\pi^*_{C=C}$ character with an excitation energy of 6.55 eV (190 nm) and an oscillator strength of 0.352. Mendez *et al.* calculated the same transition energies to be 4.7 eV and 6.3 eV.[8] Interestingly, high resolution VUV spectroscopy on aqueous acrylate conducted by the same authors showed the two transitions to be about 0.4 eV higher than those predicted by theory, namely at

Department of Chemistry, Aarhus University, Langelandsgade 140, DK-8000 Aarhus C, Denmark. E-mail: frj@chem.au.dk

5.22 eV and 6.637 eV, respectively.[8] Experimental studies of gas-phase acrylic acid suggest that photoexcitation of the $\pi^*_{CO} \leftarrow \pi_{CO}$ transition leads to the dissociation of acrylic acid along one or more of the following reactions, with reaction (4) forming CO_2 as the dominating channel:[11–17]

$$h\nu + H_2C{=}CHCOOH \rightarrow H_2C{=}CHCO^{\bullet} + OH^{\bullet} \quad (1)$$

$$\rightarrow H_2C{=}CH^{\bullet} + HOCO^{\bullet} \quad (2)$$

$$\rightarrow H_2C{=}CHOH + CO \quad (3)$$

$$\rightarrow H_2C{=}CH_2 + CO_2 \quad (4)$$

In the present work, we utilize femtosecond transient absorption spectroscopy and two-dimensional infrared (2D-IR) spectroscopy supported by density functional theory (DFT) to determine the primary reactions of aqueous acrylate following $\pi^*_{CO} \leftarrow \pi_{CO}$ photoexcitation at 6.2 eV. The high time resolution enables the identification of the primary photoreactions of acrylate before secondary reactions with other acrylate molecules or products from other photoexcitation sites have time to occur.

Experimental methods

We use the experimental technique of UV pump–IR probe transient absorption spectroscopy to record the primary photo-dynamics of aqueous acrylate following photoexcitation at 200 nm. The beam of 200 nm pump pulses used for exciting the sample is generated by frequency quadrupling a beam of 800 nm femtosecond laser pulses from an amplified Titanium:-Sapphire laser in three consecutive β-barium borate crystals. Pump pulses with an energy of 2 μJ are sent *via* a scanning delay line and through a half-wave plate before they are focused to a spot-size of 0.2 mm on the sample by a concave mirror. A mechanical chopper modulates the beam of pump pulses such that every second pump pulse excites the sample, while the rest are blocked. The beam of infrared probe pulses is generated by difference frequency mixing of the signal and idler pulses from an optical parametric amplifier pumped by the amplified Titanium-Sapphire laser. The beam of probe pulses is divided into a signal and reference beam by a beam splitter and focused onto the sample by an off-axis paraboloidal mirror. The pulses in the signal beam probe the sample inside the volume excited by the pump pulses, while the reference beam passes through the sample outside the volume excited by the pump beam. A second off-axis paraboloidal mirror recollimates the signal and reference beams, and the probe pulses are subsequently analyzed and detected by a spectrometer equipped with a dual array HgCdTe detector. The spectrum of the signal pulses is normalized to that of the reference pulses, and the transient induced absorption spectrum is obtained by subtracting the normalized probe spectrum recorded with pump pulse excitation from the normalized probe spectrum recorded without pump pulse excitation.

The samples consist of a constantly flowing wire-guided film of 0.05 M aqueous sodium acrylate. The flow ensures a fresh sample for every probe pulse and frequent replacement of the sample minimizes the buildup of permanent photoproducts and polymers. The transient absorption measurements use H_2O as the solvent except for the measurements recorded in the spectral range of 1500–1750 cm^{-1}, where the absorption associated with the H_2O bending transition renders the sample opaque. D_2O is used as the solvent in the 1500–1750 cm^{-1} range. The transient absorption measurements are recorded with pump and probe polarizations at the magic angle (54.7°). The data measured for $-0.5 < t < 0.5$ ps are obscured by the $t = 0$ ps coherence signal, and the transient absorption spectra therefore only show data after $t > 0.5$ ps. The spectral resolution of the transient absorption spectrometer is $\sim$10 cm^{-1} in the spectral range of 900–1800 cm^{-1} and $\sim$4 cm^{-1} in the range of 2100–2400 cm^{-1}. The linear pump-induced water solvent background signal has been subtracted from all transient absorption data.

We furthermore investigate the intra-molecular coupling of the vibrational modes of acrylate with a commercial 2D-IR spectrometer from Phasetech.[18,19] The mid-infrared pump and probe pulses in the 2D-IR spectrometer are generated by difference frequency mixing of the infrared pulses from an optical parametric amplifier pumped by a femtosecond Yb:KGW laser, all from light conversion. The output pump pulses are fed into a pulse shaper to produce pulse pairs with tunable delay times and phases. The delay between the pump and probe pulses is varied with a motorized delay stage in the range from 0 to 10 ps. All measurements are performed using a 4-phase cycling scheme to suppress scattering. To improve the signal-to-noise ratio, 20 scans are performed for each spectrum and averaged. The measurements are performed with parallel, $\Delta A_{\parallel}$, as well as perpendicular, $\Delta A_{\perp}$, pump and probe beam polarizations. The samples used for these measurements consist of 0.050 M acrylate dissolved in D_2O. The samples are placed between two 2 mm thick CaF_2 windows with a spacing of 100 μm. The spectrometer is purged with nitrogen throughout the measurements.

The UV-vis spectra of aqueous acrylate are recorded using a Shimadzu UV-3600 spectrometer. The steady state IR spectra are recorded by ATR FTIR with the resolution set to $\Delta\nu = 4$ cm^{-1} on a Nicolet 380 spectrometer from Thermo Fisher.

Computational details

All calculations have been done using the ωB97X-D functional,[20] the aug-pcseg-1 basis set[21] and the IEFPCM implicit solvent model.[22] The ωB97X-D includes a range-separated X-functional and empirical dispersion, with the former important to accurately describe possible charge-transfer characteristics of the excited states and the latter important for describing the interaction with explicit water molecules. Excitation energies have been calculated within the TDDFT framework, where only the optical part of the dielectric constant in the IEFPCM model is included. The effects of including up to four explicit water molecules to provide hydrogen bonding have been probed. All calculations have been performed using the Gaussian-16 software package.[23]

Results and discussion

Aqueous acrylate's UV and IR absorption spectra

Fig. 1a and b show that the ultraviolet absorption spectrum of acrylate dissolved in H_2O exhibits a strong absorption around 200 nm with an extinction coefficient of $\varepsilon(200\ \text{nm}) = 6.5(\pm0.5) \times 10^3$ l mol^{-1} cm^{-1} and a weak absorption with $\varepsilon(260\ \text{nm}) = 80(\pm10)$ l mol^{-1} cm^{-1} around 260 nm. According to our calculations, the absorption spectrum of acrylate comprises a $\pi^*_{CO} \leftarrow \pi_{CO}$ transition at 206 nm (6.0 eV) with an oscillator strength of 0.0317 from the $^1A'$ ground state to an excited state with $^1A'$ symmetry and two $\pi^*_{CO} \leftarrow n_O$ transitions at 258 nm (4.8 eV) and 247 nm (5.0 eV) with low oscillator strengths ($\sim$0.0001) to excited states with $^1A''$ symmetry. The $\pi^*_{CO} \leftarrow \pi_{CO}$ transition is thus accessible in aqueous solutions, and we investigate the photolysis of aqueous acrylate after excitation at 200 nm (6.2 eV).

Following excitation, the photo products are identified by probing the infrared absorption of the sample. The identification of the actual chemical species responsible for the observed vibrational transitions requires external calibration, which can be either experimental for stable species or calculated spectra for transient intermediates. Fig. 1c shows the measured equilibrium infrared absorption spectra of acrylate in H_2O and D_2O between 800 cm^{-1} and 2000 cm^{-1}. The vibrational transition frequencies in Fig. 1c are essentially independent of the solvent, and we only quote the frequencies recorded in H_2O. The assignments to vibrational modes are guided by comparison with calculated transition frequencies (Table S1). The absorption at 1640 cm^{-1} is assigned to the fundamental C=C stretch transition, the absorption at 1542 cm^{-1} is assigned to the fundamental asymmetric CO stretch transition of the carboxylate group, while the absorption at 1427 cm^{-1} and 1361 cm^{-1} is associated with fundamental transitions of the CH_2 scissor and symmetric CO stretch vibrations, respectively. The two absorption peaks at 1278 cm^{-1} and 1062 cm^{-1} are associated with the fundamental transitions of the CH deflection and CH_2 rock vibrations, and the peaks at 991 cm^{-1} and 964 cm^{-1} pertain to the fundamental transitions in the CH_2 wag and CH_2 twist vibrations.

Transient infrared absorption dynamics of acrylate

The primary photochemistry of aqueous acrylate is investigated by recording transient absorption spectra of the photo products between 900 cm^{-1} and 2400 cm^{-1} during the first 560 ps after driving the $\pi^*_{CO} \leftarrow \pi_{CO}$ transition with the 200 nm excitation pulse. Fig. 2 and Fig. S1 show the absorption dynamics on a logarithmic and linear timescale, respectively. Negative ΔA values imply the excitation of ground state acrylate molecules, while positive ΔA values indicate the formation of new species. The transients drop to a minimum immediately after the excitation pulse and then recover to about half of their initial value after 100 ps. The sub-picosecond drop in the transient absorption reflects the photo-induced transition of acrylate molecules from the electronic ground state to the excited electronic state. The subsequent absorption recovery signifies the return of the excited acrylate molecules to an equilibrated population distribution of the vibration levels in the electronic ground state. For some of the ground state transition frequencies, the absorption from returning acrylate anions is superimposed on

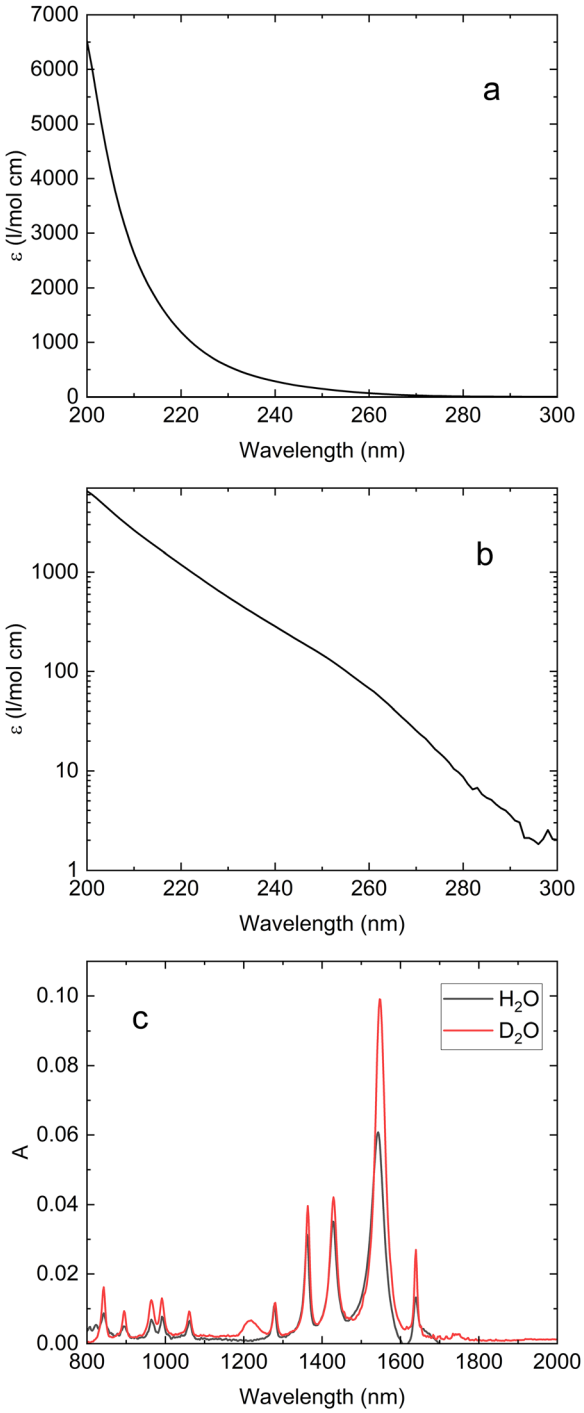

Fig. 1 Ultraviolet and infrared absorption spectra of aqueous acrylate. (a) UV absorption spectrum of aqueous acrylate recorded against an H_2O reference shown on a linear absorption scale. (b) UV absorption spectrum of acrylate dissolved in H_2O recorded against H_2O shown on a logarithmic absorption scale. The absorption scales in (a) and (b) have been calibrated to the extinction coefficients reported in ref. 23. (c) IR steady state absorption spectra of acrylate dissolved in H_2O and D_2O recorded against H_2O and D_2O references.

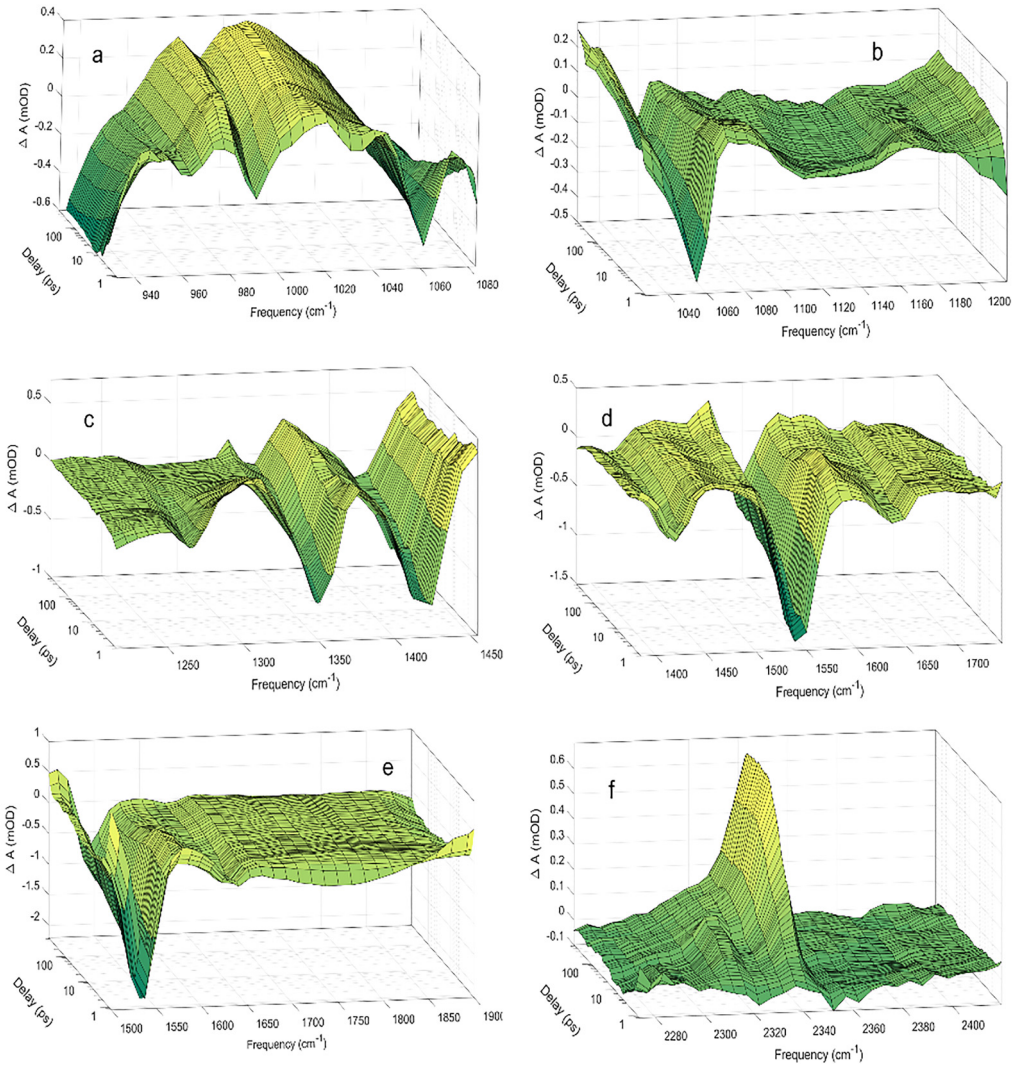

Fig. 2 The transient absorption spectra of aqueous acrylate recorded as a function of time after the 200 nm excitation pulse. (a) The negative transients at 964 cm^{-1}, 991 cm^{-1} and 1062 cm^{-1} are respectively associated with the fundamental transitions of the CH_2 twist, wag and rock vibrations of ground state acrylate. The wide positive absorption with a maximum at ~1000 cm^{-1} is assigned to ethene. (b) The negative transient at 1062 cm^{-1} is associated with the fundamental transition of CH_2 rock. (c) The negative transients at 1278 cm^{-1}, 1361 cm^{-1} and 1427 cm^{-1} are associated with fundamental transitions of the CH deflection, symmetric CO stretch and CH_2 scissor vibrations of ground state acrylate, respectively. The wide positive absorption peak observed at ~1370 cm^{-1} is assigned to the ethenyl radical. (d) The negative absorption at 1427 cm^{-1} is associated with the excitation of the CH_2 scissor vibration, while the negative absorptions at 1542 cm^{-1} and 1640 cm^{-1} pertain to the fundamental asymmetric CO stretch and C=C stretch vibration of ground state acrylate, respectively. The positive absorption appearing at ~1515 cm^{-1} is assigned to the ethenyl radical. (e) No additional transients. (f) The positive transient at 2341 cm^{-1} is assigned to aqueous CO_2. The positive absorption transients on the low frequency side of all the negative absorption transients are associated with vibrationally relaxing acrylate molecules returning to the electronic ground state after the photoexcitation. The transient spectra depicted in (a)–(c) and (f) are recorded using H_2O as the solvent, while (d) and (e) are recorded using D_2O. The transient spectra cannot be compared on a common scale.

the absorption pertaining to the formation of photoproducts. Fig. 3 shows the ground state absorption recovery exemplified by the asymmetric CO_2^- stretch transient at 1542 cm^{-1} for the first 250 ps. If the data are fitted by a double exponential function, the best agreement is obtained with time constants of 5.0 ± 0.4 ps and 67 ± 45 ps for the major (83%) and minor (17%) components of the recovery. The high uncertainty of the latter time constant reflects the non-exponential behavior of the minor absorption recovery component. Due to the anharmonicity of the acrylate ground state potential, the vibrationally excited molecules returning to the electronic ground state after photoexcitation absorb at lower frequencies than molecules in the equilibrated ground state. As the acrylate molecules relax with time, the absorption shifts towards higher frequencies and merges with the ground state absorption in ~5 ps. Hydration of the returning molecules further adds to the spectral shift. Inspection of the low frequency side of all the negative absorption transients in Fig. 2 reveals a positive absorption transient lasting for a few picoseconds with the spectral dynamics characteristics of molecules relaxing towards the equilibrated ground state.

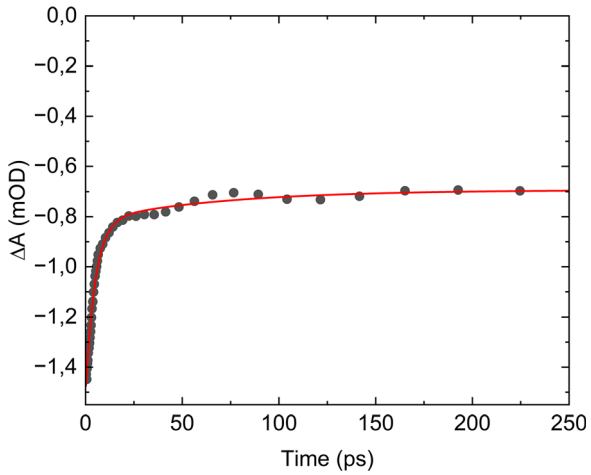

Fig. 3 Acrylate ground state absorption recovery exemplified by the first 250 ps of the transient recorded at 1542 cm^{-1}. The data are fitted by a double exponential function ΔA (t, 1542 cm^{-1}) = 0.62 exp(−t/5.0 ps) + 0.13 exp(−t/67 ps) - 0.069 mOD with time constants of 5.0 ± 0.4 ps and 67 ± 45 ps.

2D-IR spectra of aqueous acrylate

Vibrational relaxation redistributes the excess energy among the vibrational modes of acrylate in competition with vibrational energy dissipation to the surrounding water molecules. The electronic coupling of the conjugated C═C and C–CO_2^- bonds likely implies a strong vibrational coupling leading to an efficient intra-molecular energy redistribution. The strong coupling between the carboxylate anion and the surrounding polar water molecules furthermore suggests an efficient intermolecular energy dissipation to the solvent. To investigate the intra- and inter-molecular energy dissipation of the C═C and CO_2^- vibrations, we have recorded the 2D-IR spectrum of acrylate from 1500 cm^{-1} to 1680 cm^{-1}. The 2D-IR spectrum in Fig. 4 shows the pump–probe absorption spectrum as a function of pump frequency recorded with parallel pump and probe polarizations after delays of 0 fs (Fig. 4a) and 500 fs (Fig. 4b) between the pump and probe pulses. The infrared absorption spectrum from Fig. 1c is reflected in the negative (blue) ground state absorption minima on the diagonal, and the positive (red) maxima beside them show the induced excited state absorption. Off-diagonal extrema pairs reveal coupling between the two vibrations. The 2D-IR spectrum of acrylate shows just two diagonal features: the asymmetric carboxylate stretch around 1556 cm^{-1} and the C═C stretch around 1640 cm^{-1}. As expected, the off-diagonals (1640 cm^{-1}, 1556 cm^{-1}) and (1556 cm^{-1}, 1640 cm^{-1}) show a substantial coupling between the two conjugated bonds, which facilitates the intra-molecular transfer of vibrational energy. To gauge the efficiency of this transfer and compare it to the energy dissipation from the carboxylate group to water, we have measured the relaxation time of the two vibrational modes from several time-resolved 2D-IR spectra recorded at different time delays between pump and probe pulses. Fig. 5a and b show how the isotropic absorption ($\Delta A_{iso} = 2\Delta A_{\perp} + \Delta A_{\parallel}$) of the diagonal features in the 2D-IR spectra changes with time. Fig. 5a shows that when the fundamental asymmetric stretch of the carboxylate group is excited at 1556 cm^{-1}, its return to the ground state is well described by a single exponential decay with a time constant of 0.43 ± 0.06 ps. Fig. 5b shows that when the fundamental C═C stretch is excited at 1640 cm^{-1}, it relaxes to the ground state in 3.1 ± 0.6 ps – approximately 7 times slower compared with the carboxylate. Fig. 5c shows that the coupling of the two modes represented by off-diagonal absorption decays in 2.5 ± 1 ps reflects the slower relaxation of the C═C stretch. Energy transfer from the carboxylate group to water thus dominates the energy dissipation from vibrational states close to the vibrational ground state. Considering that the vibrational coupling increases as the potential energy surface becomes more anharmonic, the intramolecular vibrational coupling is expected to increase with excitation energy. Furthermore, anharmonicity lowers the vibrational transition energies, thereby increasing the overlap with energy accepting libration modes of water.[24] The relaxation of highly excited vibrational levels is therefore expected to be even faster than the fundamental transitions recorded by 2D-IR spectroscopy. Altogether this explains how acrylate anions returning to the electronic ground state dissipate their excess energy and equilibrate with the solvent on a time scale of only 5 ps. Fig. 5d shows the rotational anisotropy of acrylate. It is interesting to note that

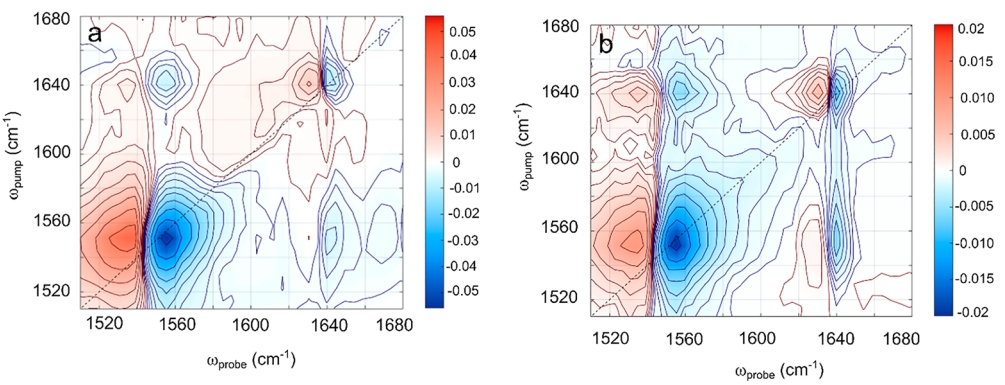

Fig. 4 The 2D-IR spectra of acrylate from 1500–1680 cm^{-1} recorded with parallel pump and probe polarizations after time delays of 0 fs (a) and 500 fs (b) between the pump and probe pulses.

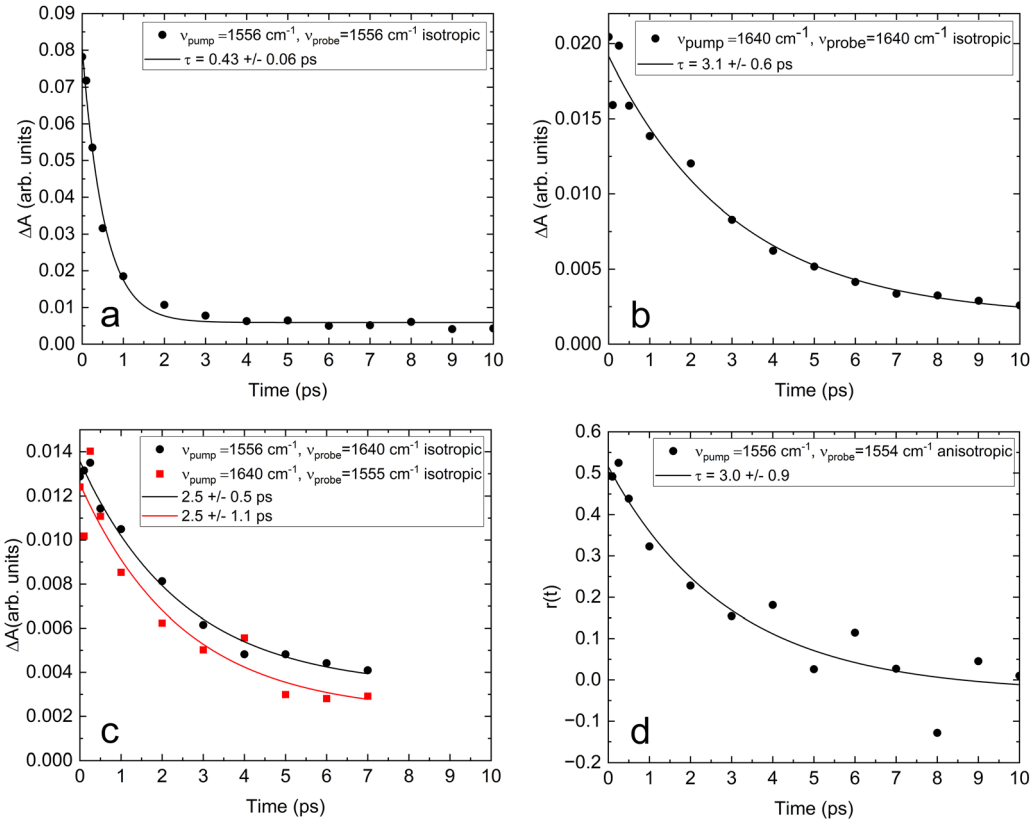

Fig. 5 Vibrational relaxation profiles for fundamental C=C stretch of acrylate at (1640 cm^{-1}, 1640 cm^{-1}) (a), CO stretch at (1556 cm^{-1}, 1556 cm^{-1}) (b), and the cross peak at (1640 cm^{-1}, 1556 cm^{-1}) (c). The relaxation dynamics fit with a single exponential function (red line) to obtain the vibrational relaxation lifetimes for the ground state transitions of aqueous acrylate. The anisotropic signal $\Delta A_{aniso} = (\Delta A_{\parallel} - \Delta A_{\perp})/(2\Delta A_{\perp} + \Delta A_{\parallel})$ recorded on the carboxylate transition shows that the acrylate anion rotates in water on a time scale of 3.0 ± 0.9 ps (d).

the anisotropic signal $\Delta A_{aniso} = (\Delta A_{\parallel} - \Delta A_{\perp})/(2\Delta A_{\perp} + \Delta A_{\parallel})$ recorded on the carboxylate transition shows that the acrylate anion rotates in water on a similar time scale of 3.0 ± 0.9 ps.

Photoproducts

In addition to the absorption associated with the excitation and subsequent return of ground-state acrylate, Fig. 2 shows several positive absorption transients indicating the formation of new species. Central to the primary photochemistry of acrylate is the observation of the positive absorption transients pertaining to the $\nu_3 = 1 \rightarrow 2$ hot band of the CO_2(aq) asymmetric stretch transition at 2314 cm^{-1} and the fundamental CO_2(aq) asymmetric stretch $\nu_3 = 0 \rightarrow 1$ transition at 2341 cm^{-1} in Fig. 2f.[25–28] The identification of CO_2 shows that part of the photoexcited acrylate anions dissociate by decarboxylation. The decarboxylation of aqueous acrylate is equivalent to the decarboxylation of gas-phase acrylic acid (reaction (4)) observed experimentally.[11–17] The absorption trace recorded at 2341 cm^{-1} is depicted in Fig. 6 and shows that the absorption associated with ground state CO_2 is initially absent but then increases to a constant level within 50 ps. The absorption trace is well described by a single exponential function with a time constant of τ = 10.4 ± 0.3 ps. It is hard to imagine a dissociation process being so slow and the explanation for the slowly increasing absorption pertaining to the asymmetric stretch of CO_2 is more likely related to the geometry of the dissociating CO_2 fragment. Upon dissociation from acrylate, the CO_2 fragment is transformed from its bent geometry in the carboxylate anion to the linear geometry of the equilibrated CO_2 molecule. Consequently, probing the aqueous acrylate sample at transition

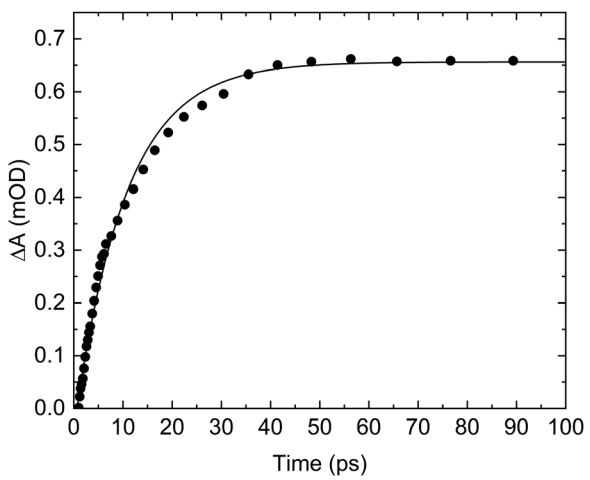

Fig. 6 The absorption trace recorded at 2341 cm^{-1} associated with ground state CO_2. The first 100 ps of the absorption trace is well described by a single exponential function with a time constant of τ = 10.4 ± 0.3 ps.

frequencies associated with the asymmetric stretch of the linear CO_2 molecule shows no absorption initially. As the bent CO_2 fragment leaves its counter product at the dissociation site, it gradually assumes its linear geometry with its associated transition frequencies and intensities. During this process, the excess energy of the dissociating CO_2 fragment is dissipated to the solvent through vibrational relaxation first in the bending mode and later also in the asymmetric stretch mode. Since the bending transitions are outside the range of our transient absorption spectrometer, we are unable to follow the vibrational relaxation of the bent fragment, but as the CO_2 fragment approaches its linear geometry, we observe the relaxation in the asymmetric stretch, first by the transition associated with the $\nu_3 = 1 \rightarrow 2$ hot band of the CO_2(aq) asymmetric stretch at 2314 cm^{-1} and eventually by the fundamental transition at 2341 cm^{-1}. The $\nu_3 = 1 \rightarrow 2$ hot band is only barely visible in Fig. 2f, consistent with the relaxation predominantly taking place in the bending mode. We have previously observed similar absorption dynamics of CO_2(aq)'s asymmetric stretch transition following the photodecarboxylation of a number of carboxylates, amino acid zwitterions and di-peptides, suggesting a common CO_2 vibrational relaxation path for these molecules.[29–33] The relatively slow relaxation of CO_2 is in line with the weak interaction between CO_2 and its hydration shell reported by previous studies.[34] Hence, the delayed appearance of the CO_2 infrared absorption likely reflects the relaxation towards the linear ground state geometry, while decarboxylation itself occurs within a few picoseconds after the photoexcitation. We return to the decarboxylation dynamics when we have identified CO_2's counter product below. As our spectrometer is unable to cover the positive CO_2(aq) absorption transient at 2341 cm^{-1} simultaneously with any of the negative absorption transients associated with the excitation of acrylate in one measurement, we are unable to determine the quantum yield of CO_2 from this measurement. For comparison, following the photo-excitation of gas-phase acrylic acid at 193 nm and 249 nm, Rosenfeldt and Weiner[11] recorded a unity decarboxylation (reaction (4)). Owing to a 7 μm detector cut-off, they were unable to detect the excitation of the CO_2 bending mode but found that after an instrument limited rise time of 1 μs, CO_2 was vibrationally excited in the asymmetric stretch.

The formation of CO_2 entails the CH_2CH^- counter product, which is a strong base and likely forms ethene, $H_2C{=}CH_2$ ($H_2C{=}CHD$), upon abstracting a proton (deuteron) from water. The identification of ethene in the transient absorption data is hampered by the lack of an IR spectrum of aqueous ethene. Our attempts to measure this spectrum failed, as we were unable to dissolve detectable amounts of ethene in water. Since the interaction between the non-polar ethene and the polar water is expected to be weak, we instead relied on using ethene's gas-phase spectrum. The gas-phase spectrum has a relatively strong (I = 84 km mol^{-1} [35]) and wide absorption centered at 980 cm^{-1} associated with the CH_2 out-of-plane wagging and an ~10 times weaker (I = 8 km mol^{-1} [35]) absorption at 1413 cm^{-1} associated with the fundamental transition of HCH in-plane scissoring. In the spectral region where D_2O is used as the solvent, the $H_2C{=}CHD$ isotopomer reduces the symmetry from D_{2h} to C_s, thereby allowing the fundamental C=C stretch transition at 1600 cm^{-1} symmetry, but the calculated intensity of 0.3 km mol^{-1} is two orders of magnitude lower than that of the 980 cm^{-1} transition.[35] Assuming the same intensities apply to aqueous solutions, ethene is a viable candidate for the wide positive transient absorption observed around 1000 cm^{-1}, while ethene's transition expected at 1413 cm^{-1} will be dominated by the negative absorption associated with acrylate's CH_2 in-plane scissoring transition at 1427 cm^{-1} and the C=C stretch transition expected at 1600 cm^{-1} is below the instrument detection limit. The identification of ethene thus hinges on one transition only. To further investigate if the assignment to ethene is correct, we have recorded the transient absorption spectrum of acrylate in D_2O in the range from 940 cm^{-1} to 1080 cm^{-1} to see if the corresponding $H_2C{=}CHD$ isotopomer is formed. In accordance with gas-phase spectroscopy,[36] our calculations (Table S2) indicate that the strong CH_2 out-of-plane wagging transition of $H_2C{=}CH_2$ at 980 cm^{-1} splits into two weaker transitions at 835 cm^{-1} and 985 cm^{-1} associated with the CHD and CH_2 out-of-plane wagging of $H_2C{=}CHD$. Fig. S2 compares the transient absorption data of acrylate recorded in H_2O and D_2O. In agreement with the predictions for ethene, the comparison clearly shows that the strong transient absorption of $H_2C{=}CH_2$ observed at 980 cm^{-1} is replaced by a significantly weaker transient absorption when H_2O is replaced by D_2O. The transition at 835 cm^{-1} is beyond the reach of our transient absorption spectrometer. No other conceivable counter product to CO_2 matches the measured transient absorption data. Hence, we assign the absorption dynamics at 980 cm^{-1} to ethene and further discuss additional counter products to CO_2 below. Fig. 2a shows that the absorption pertaining to ethene already reaches its final value in $<$0.8 ps and remains constant thereafter. This has two important consequences. First, the photodecarboxylation of acrylate and subsequent proton abstraction from H_2O occur in less than 0.8 ps. The decarboxylation of acrylate is thereby an order of magnitude faster than acrylate's relaxation to the ground state, implying that the decarboxylation likely occurs from electronically excited states rather than the acrylate ground state. Second, the yield of ethene produced after 0.8 ps by other reactions must be insignificant.

The formation of CO_2 could also involve the production of solvated electrons by the reaction $h\nu + H_2C{=}CHCOO^- \rightarrow H_2C{=}CH^\bullet + CO_2 + e^-$. The ethenyl radical, $H_2C{=}CH^\bullet$, is less prone to react with water than $H_2C{=}CH^-$ and possibly has a longer lifetime than the anion before forming ethene. If the formation dynamics of $H_2C{=}CH^\bullet$ are to be consistent with the transient absorption dynamics observed for CO_2 and $H_2C{=}CH_2$, $H_2C{=}CH^\bullet$ radicals produced by this reaction must appear in 0.8 ps and persist for the 560 ps duration of the measurements. The infrared absorption of aqueous $H_2C{=}CH^\bullet$ is unknown, but according to measurements in solid noble gas matrices, $H_2C{=}CH^\bullet$ absorbs at 898 cm^{-1} and 1339–1360 cm^{-1}.[37,38] Ref. 35 also tentatively assigns a transition at 1585 cm^{-1} to $H_2C{=}CH^\bullet$. The absorption from $H_2C{=}CH^\bullet$ expected at 898 cm^{-1} is out of reach of our transient absorption

spectrometer. The absorption expected at 1339–1360 cm^{-1} and 1585 cm^{-1} matches the frequencies of the absorption transients observed at 1368 cm^{-1} and 1585 cm^{-1}, but the absorption dynamics at 1368 cm^{-1} and 1585 cm^{-1} are different and unlikely to come from the same species. Moreover, the absorption dynamics of the two transients conflict with the restrictions imposed by the transient absorption of $H_2C{=}CH_2$ and CO_2. Consequently, decarboxylation by the reaction $h\nu$ + $H_2C{=}CHCOO^- \rightarrow H_2C{=}CH^\bullet + CO_2 + e^-$ is insignificant. The lack of $H_2C{=}CH^\bullet$ also excludes the reaction $h\nu$ + $H_2C{=}CHCOO^- \rightarrow H_2C{=}CH^\bullet + CO_2^-$ where the electron stays on the CO_2 fragment forming CO_2^- (equivalent to reaction (2)). The fact that the absorption associated with the asymmetric stretch of CO_2^- at 1637 cm^{-1} is missing in the transient absorption data further supports this assessment.[39]

In addition to decarboxylation, aqueous acrylate could dissociate as $h\nu + H_2C{=}CHCOO^- \rightarrow H_2C{=}CHO^- + CO$, equivalent to reaction (3) for gas-phase acrylic acid. If so, $H_2C{=}CHO^-$ will subsequently be protonated by water to form vinyl alcohol, $H_2C{=}CHOH/D$,[40] which, with time, forms an enol–keto equilibrium with acetaldehyde. Alternatively, acetaldehyde could be formed directly. According to our calculations (Table S3), aqueous $H_2C{=}CHO^-$ has three strong transitions at 1309 cm^{-1}, 1398 cm^{-1} and 1573 cm^{-1} in addition to weaker transitions at 951 cm^{-1}, 979 cm^{-1}, and 1217 cm^{-1}. The calculated frequencies of the three strong transitions are in fair agreement with the three short-lived transients observed at 1316 cm^{-1}, 1377 cm^{-1} and 1585 cm^{-1}. The three transients sit between the steep flanks of the negative absorption from acrylate, which may shift the absorption maxima from the actual transition frequencies by $\sim$10 cm^{-1} and perturb the absorption dynamics. Of the three, the transient absorption at 1316 cm^{-1} is least affected by overlapping absorption transients and is shown in detail in Fig. S3. The absorption is already at its maximum in $<$0.8 ps after the photoexcitation of acrylate and decays with a time constant of 16 $\pm$ 4 ps, presumably indicating the protonation to vinyl alcohol. Spectroscopy studies on vinyl alcohol in argon matrices report strong transitions at 1075–1079 cm^{-1} and 1117–1121 cm^{-1} for $H_2C{=}CHOH$ and at 1621–23 cm^{-1} and 1662 cm^{-1} for $H_2C{=}CHOD$.[40] The transient absorption spectra in Fig. 2b and d show four weak absorption transients at matching frequencies, thus supporting the suggested reaction scenario (see Fig. S4 and S5 for detailed views). The quantitative assessment of the dynamics of the four absorption transients is hampered by overlapping absorption from other species. The spectrally most isolated of the four transitions is the one observed around 1110 cm^{-1}. This absorption becomes discernible from the absorption from other species after $\sim$20 ps and increases throughout the rest of the measurement in line with the suggested protonation. The data show no sign of the strong carbonyl transition of acetaldehyde at 1716 cm^{-1} (see Fig. S6), indicating that the suggested enol–keto reaction is insignificant during the first 560 ps after the photoexcitation of acrylate. The formation of $H_2C{=}CHO^-$ and subsequently $H_2C{=}CHOH/D$ implies the formation of the CO and OH^-/OD^- counter products. The single transition of CO(aq) at 2146 cm^{-1} is not identified in the transient absorption data (Fig. S7).[41] However, the oscillator strength of CO(aq) is weak and CO(aq) would likely be undetectable even if produced in high yield. Although these data compare favorably to the reactions $h\nu + H_2C{=}CHCOO^- \rightarrow H_2C{=}CHO^- + CO$ and subsequently $H_2C{=}CHO^- + H_2O \rightarrow H_2C{=}CHOH + OH^-$, the assignment of some of the observed transitions is not unique and vinyl alcohol may be formed by other reactions, as we will show next.

Photoexcitation of aqueous acrylate may also lead to the reaction $h\nu$ + $H_2C{=}CHCOO^- \rightarrow H_2C{=}CHO^\bullet + CO^-$. $H_2C{=}CHO^\bullet$ is expected to abstract a hydrogen from a neighboring water molecule and form vinyl alcohol, $H_2C{=}CHOH/D$,[40] which in turn forms an enol–keto equilibrium with acetaldehyde. The calculated transition frequencies of $H_2C{=}CHO^\bullet$ at 1165 cm^{-1}, 1386 cm^{-1}, 1465 cm^{-1} and 1577 cm^{-1} (Table S4) are all in fair agreement with short-lived ($\sim$20–30 ps) absorption transients observed at 1180 cm^{-1}, 1368 cm^{-1}, 1462 cm^{-1} and 1585 cm^{-1} (see Fig. 2c and d and Fig S4 and S5). The transient nature of the $H_2C{=}CHO^\bullet$ radical agrees with the subsequent formation of $H_2C{=}CHOH/D$,[40] which appears as $H_2C{=}CHO^\bullet$ disappears. This reaction channel implies the formation of CO^-. To the best of our knowledge, the absorption spectrum of CO^-(aq) is unknown. The calculated fundamental transition of CO^-(aq) is 1640 cm^{-1} (Table S5) with an intensity comparable to that of the strongest transitions of ground state acrylate (Table S1). Considering the uncertainty of our calculations and spectral resolution of the transient spectrometer, the calculated transition frequency of 1640 cm^{-1} coincides with that of the acrylate ground state C=C stretch at 1640 cm^{-1} and, if present, it likely contributes to the weak absorption measured at 1662 cm^{-1}. The absorption at 1662 cm^{-1} is too intertwined with the negative absorption from the acrylate ground state C=C stretch to assess its dynamics and it neither confirms nor refutes the reaction. The experimental data thus suggest that vinyl alcohol can be formed from both the reactions $H_2C{=}CHO^- + H_2O \rightarrow H_2C{=}CHOH + OH^-$ and $H_2C{=}CHO^\bullet + H_2O \rightarrow H_2C{=}CHOH + OH^\bullet$.

The reaction channel corresponding to reaction (1), $h\nu$ + $H_2C{=}CHCOO^- \rightarrow H_2C{=}CHCO + O^-$, on the other hand, is incompatible with the measured transient absorption data because the strong C=O stretch transition with a calculated value of 1869 cm^{-1} (Table S6) has no match in the experimental data. If at all present, the reaction $h\nu$ + $H_2C{=}CHCOO^- \rightarrow H_2C{=}CHCO + O^-$ is therefore only a minor reaction channel. Neither is the transient absorption data compatible with the calculated transitions of the lowest excited triplet state (Table S7). Hence, intersystem crossing is not observed, and the primary photochemistry of acrylate thus takes place from the excited singlet state.

Conclusion

The efficient $\pi^*_{CO} \leftarrow \pi_{CO}$ photoexcitation of aqueous acrylate at 200 nm resulting from acrylate's conjugation leads to rich

primary and secondary chemistry in which water plays a decisive part as a reactant and an energy acceptor. Upon the photoexcitation of acrylate about half of the excited anions return to the ground state and relax to equilibrium in 5 ps primarily through strong intermolecular coupling between the carboxylate group and the surrounding water. The rest of the excited molecules dissociate. Three dissociation channels have been identified. Perhaps the most prominent primary reaction is decarboxylation of acrylate, forming CO_2 and CH_2CH^-. Upon dissociation, CO_2 assumes the bent geometry of the carboxylate group, which slowly relaxes on a 10 ps timescale to the linear configuration of ground state CO_2, indicating weak coupling to the surrounding water molecules. CH_2CH^- picks up a proton from water and forms ethene in less than 0.8 ps. In the second photo reaction, acrylate dissociates to $H_2C{=}CHO^-$ and CO and on a time scale of about 20 ps, ($H_2C{=}CHO^-$) attracts a proton from water to produce vinyl alcohol, $H_2C{=}CHOH$. In a third possible dissociation channel, the electron is associated with the CO group, forming $H_2C{=}CHO^\bullet$ and CO^-, and $H_2C{=}CHO^\bullet$ abstracts a hydrogen from a neighboring water molecule to again form vinyl alcohol. Vinyl alcohol will tautomerize to acetaldehyde, but this occurs on a time scale longer than the experimental observation time of 0.56 ns. These relatively direct photochemical pathways to CO_2, ethene, and acetaldehyde formation suggest that acrylate photodissociation may be a previously underestimated source of reactive carbon species and small organics in aerosols, sea spray and surface waters, with implications for secondary organic aerosol formation and photochemical cycling in the environment.

Author contributions

F. J. suggested the project. J. T. designed and directed the project. J. T. recorded and analyzed the stationary and transient absorption data. A. M. recorded and analyzed the 2D-IR data. F. J. provided the theoretical calculations. J. T. and F. J. interpreted the data and wrote the manuscript with help from A. M. and T. W.

Conflicts of interest

The authors declare no competing interests.

Data availability

Relevant data are included in the SI. Supplementary information is available. See DOI: **https://doi.org/10.1039/d5cp03023d**.

Acknowledgements

T. W. and J. T. acknowledge the Novo Nordisk Foundation Facility Grant NanoScat No. NNF18OC0032628, the Novo Nordisk Foundation (New Exploratory Research and Discovery – NERD Grant, NNF22OC0074640), and the Danish National Research Foundation (DNRF172) through the Center of Excellence for Chemistry of Clouds for funding. The authors thank Ditte Thomsen for help with the TOC.

References

1 Y. Meng, Y. Xia, J. Xu and R. Zare, *Sci. Adv.*, 2025, **11**, 2375.
2 A. Kumar, V. S. Avadhani, A. Nandy, S. Mondal, B. Pathak, V. K. N. Pavuluri, M. M. Avulapati and S. Banerjee, *Anal. Chem.*, 2024, **96**, 10515.
3 G. M. Hale and M. R. Querry, *Appl. Opt.*, 1973, **12**, 555.
4 B. Budac and P. Wan, *J. Photochem. Photobiol., A*, 1992, **67**, 135.
5 T. J. A. Wolf, R. H. Myhre, J. P. Cryan, S. Coriani, R. J. Squibb, A. Battistoni, N. Berrah, C. Bostedt, P. Bucksbaum, G. Coslovich, R. Feifel, K. J. Gaffney, J. Grilj, T. J. Martinez, S. Miyabe, S. P. Moeller, M. Mucke, A. Natan, R. Obaid, T. Osipov, O. Plekan, S. Wang, H. Koch and M. Guhr, *Nat. Commun.*, 2017, **8**, 29.
6 L. Xue and D. J. Kieber, *Environ. Sci. Technol.*, 2021, **55**, 7135.
7 X. Wu, C.-Y. Liu and P.-F. Li, *Mar. Chem.*, 2015, **170**, 29.
8 M. Mendes, A. S. Barbosa, F. Ferreira da Silva, N. C. Jones, S. V. Hoffmann, G. García, M. H. F. Bettega and P. Limao-Vieira, *J. Chem. Phys., A*, 2018, **122**, 8191.
9 D. Shemesh and R. B. Gerber, *J. Phys. Chem. Lett.*, 2018, **9**, 527.
10 W.-H. Fang and R.-Z. Liu, *J. Am. Chem. Soc.*, 2000, **122**, 10886.
11 R. N. Rosenfeldt and B. R. Weiner, *J. Am. Chem. Soc.*, 1983, **105**, 6233.
12 D. C. Kitchen, N. R. Forde and L. J. Butler, *J. Phys. Chem. A*, 1997, **101**, 6603.
13 M. C. Osborne, Q. Li and I. W. M. Smith, *Phys. Chem. Chem. Phys.*, 1999, **1**, 1447.
14 H. P. Upadhyaya, A. Kumar, P. D. Naik, A. V. Sapre and J. P. Mittal, *J. Chem. Phys.*, 2002, **117**, 10097.
15 R. R. Zhang, C. C. Qin, J. Y. Long, M. H. Yang and B. Zhang, *Acta Phys.-Chim. Sin.*, 2012, **28**, 522–527.
16 A. J. Fleisher, B. J. Bjork, T. Q. Bui, K. C. Cossel, M. Okumura and J. Ye, *J. Phys. Chem. Lett.*, 2014, **5**, 2241.
17 M. F. Arendt, P. W. Browning and L. J. Butler, *J. Chem. Phys.*, 1995, **103**, 5877.
18 A. B. Thomassen, T. L. C. Jansen and T. Weidner, *Phys. Chem. Chem. Phys.*, 2024, **26**, 18538.
19 F. Madzharova and T. Weidner, *ACS Food Sci. Technol.*, 2024, **4**, 1430.
20 J.-D. Chai and M. Head-Gordon, *Phys. Chem. Chem. Phys.*, 2008, **10**, 6615.
21 F. Jensen, *J. Chem. Theory Comp.*, 2014, **10**, 1074.
22 M. J. Frisch, G. W. Trucks, H. B. Schlegel, G. E. Scuseria, M. A. Robb, J. R. Cheeseman, G. Scalmani, V. Barone, G. A. Petersson, H. Nakatsuji, X. Li, M. Caricato, A. V. Marenich, J. Bloino, B. G. Janesko, R. Gomperts, B. Mennucci, H. P. Hratchian, J. V. Ortiz, A. F. Izmaylov, J. L. Sonnenberg, D. Williams-Young, F. Ding, F. Lipparini, F. Egidi, J. Goings, B. Peng, A. Petrone, T. Henderson,

D. Ranasinghe, V. G. Zakrzewski, J. Gao, N. Rega, G. Zheng, W. Liang, M. Hada, M. Ehara, K. Toyota, R. Fukuda, J. Hasegawa, M. Ishida, T. Nakajima, Y. Honda, O. Kitao, H. Nakai, T. Vreven, K. Throssell, J. A. Montgomery, Jr., J. E. Peralta, F. Ogliaro, M. J. Bearpark, J. J. Heyd, E. N. Brothers, K. N. Kudin, V. N. Staroverov, T. A. Keith, R. Kobayashi, J. Normand, K. Raghavachari, A. P. Rendell, J. C. Burant, S. S. Iyengar, J. Tomasi, M. Cossi, J. M. Millam, M. Klene, C. Adamo, R. Cammi, J. W. Ochterski, R. L. Martin, K. Morokuma, O. Farkas, J. B. Foresman and D. J. Fox, *Gaussian-16*, Gaussian, Inc., Wallingford CT, 2016.

23 L. Xu and D. J. Kieber, *J. Photochem. Photobiol., A*, 2024, **449**, 115371.

24 C. C. Yu, K. Y. Chiang, M. Okuno, T. Seki, T. Ohto, X. Yu, V. Korepanov, H. Hamaguchi, M. Bonn, J. Hunger and Y. Nagata, *Nat. Commun.*, 2020, **11**, 5977.

25 L. H. Jones and E. McLaren, *J. Chem. Phys.*, 1958, **28**, 995.

26 M. Falk and A. G. Miller, *Vib. Spectrosc.*, 1992, **4**, 105.

27 T. Schädle, B. Pejcic and B. Mizaikoff, *Anal. Methods*, 2116, **8**, 756.

28 J. Gleim, J. Lindner and P. Vöhringer, *J. Chem. Phys.*, 2022, **156**, 094595.

29 M. M. Madsen, F. Jensen, S. J. Knak Jensen and J. Thøgersen, *Phys. Chem. Chem. Phys.*, 2019, **21**, 7358.

30 M. M. Madsen, F. Jensen and J. Thøgersen, *Phys. Chem. Chem. Phys.*, 2020, **22**, 2307.

31 J. Thøgersen, V. Vaida, M. Bregnhøj, T. Weidner and F. Jensen, *Phys. Chem. Chem. Phys.*, 2021, **23**, 4555.

32 J. Thøgersen, T. Weidner and F. Jensen, *Phys. Chem. Chem. Phys.*, 2021, **23**, 10040.

33 J. Thøgersen, A. S. Chatterley, T. Weidner and F. Jensen, *J. Am. Chem. Soc.*, 2023, **145**, 9777.

34 S. R. Zukowski, P. D. Mitev, K. Hermansson and D. Ben-Amotz, *J. Phys. Chem. Lett.*, 2017, **8**, 2971.

35 J. G. Radziszewski, V. Balaj, P. Carsky and E. W. Thulstrup, *J. Phys. Chem.*, 1991, **95**, 5064.

36 T. L. Tan and G. B. Lebron, *J. Mol Spectrosc.*, 2011, **269**, 109.

37 M. E. Jacox and W. E. Thompson, *J. Chem. Phys.*, 2011, **134**, 064321.

38 H. Tanskanen, L. Khriachtchev, M. Räsänen., V. I. Feldman, F. F. Sukhov, A. Yu. Orlov and D. A. Tyurin, *J. Chem. Phys.*, 2005, **123**, 064318.

39 J. Thøgersen, T. Weidner and F. Jensen, *Phys. Chem. Chem. Phys.*, 2023, **25**, 14104.

40 M. Rodler, C. E. Blom and A. Bauder, *J. Am. Chem. Soc.*, 1984, **106**, 4029.

41 J. Thøgersen, T. Weidner and F. Jensen, *Phys. Chem. Chem. Phys.*, 2022, **24**, 24695.

